EXPERIMENTAL AND THEORETICAL STUDY OF DYNAMIC STOCHASTICITY EFFECTS UNDER CRACK PROPAGATION IN STRUCTURES

O.B. Naimark, V.A. Barannikov, S.V. Uvarov, D.N. Naldaev

Institute of Continuous Media Mechanics
Ural Department of Russian Academy of Sciences
1 Ak. Korolev Street, 614061 Perm, Russia

SUMMARY: A theoretical and experimental study of crack propagation dynamics in PMMA is presented. The transition from a steady-state regime to a branching one and the stochastic scenario of crack propagation are investigated experimentally by considering fracture surface patterns and by high speed camera recording. We find that the mechanism for the change of the crack propagation regime is linked with the nonlinear dynamics of the microcracks ensemble at the crack tip and the formation of daughter cracks.

KEYWORDS: damage, crack, structures, localization.

INTRODUCTION

There is an upsurge of interest in the problem of crack advance through locally heterogeneous materials since o complete understanding could a key to tough materials design. As a matter of fact, microstructural elements as grain boundaries, second phase precipitation, dislocation pile-ups, microcracks are able not only to force crack deflection by modifying locally the stress intensity factor, but also to change qualitatively the mechanisms of crack dynamics due to the interaction of the main crack with ensemble of the microscopic defects. As the consequence, the progress in the understanding has been made in the development of statistical physics of the defects ensemble, in the derivation of the corresponding continuum description and in the improving of the adequate experimental technique.

Experimental study, statistical and nonlinear continuum description of the microcrack ensemble evolution allowed us to establish specific properties of the system " solid with defects " and to study the scaling laws of the transition from damage to fracture [1]. It was found that failure scaling is the consequence of collective effects in the defects (microcracks) ensemble and is caused by universal laws of considered nonlinear system. The structure evolution is accompanied by non-equilibrium kinetic transitions that lead to the generation of localized modes of failure and sharp changes of the symmetry properties (topological transitions).

Nonlinear dynamics of crack propagation is the subject of the growing interest during last decade due to the experimental observation of the dynamic stochasticity effects and the

discovery of the crack behavior that is in the strong contradiction with the traditional view in the fracture mechanics. Experiments showed the existence of the limit velocity $V_c \sim 0.4 V_R$ (V_R is the Rayleigh wave speed) for the steady-state crack propagation and the threshold character of the transition to the branching regime with the stochastic dynamics. The established experimental data revealed some unresolved puzzles from point of view of the traditional crack mechanics. The main question is concerning the nature of physical mechanisms controlling the crack dynamics including the branching. Theoretical explanation of the limiting steady-state crack velocity and the transition to the branching regime was proposed by authors [2] due to the study of the collective behavior in the microcracks ensemble at the crack tip area. These theoretical results were supported by the direct experimental study of crack dynamics in PMMA specimen with the usage of the high speed camera (1 picture-100 nanosec) that allowed us to confirm the threshold character of the transition from the steady-state to the branching regime of crack propagation at V_c and the leading role in this transition nonlinear microcracks kinetics at the crack tip. To combine the recording of the crack dynamic picture with the photo-elasticity method we visualized the stress wave pattern generated at the crack tip with the pronounced Doppler effect. The study of the of the fracture surface pattern allowed the establishment of the roughness correlation with the stress wave pattern and the topological properties of the attractor responsible for the nucleation of the daughter cracks.

STATISTICAL MODEL AND CONSTITUTIVE EQUATIONS

An adequate analysis of the failure processes as evolution of ensembles of typical mesoscopic defects (dislocation pile-ups, microcracks and microshears) is thought to be impossible without a statistical method. However this should be a statistical mechanics of a few randomly located and interacting defects, changing their dimensions and orientations in the field of external and structural stresses, but it is not the phenomenological statistics. Taking into account the experimental data concerning nucleation and growth of microcracks (variable number of interacting defects, change of their size and orientation parameters during loading) statistical description arises as complicated problem, the solution of which may present essential difficulties if not supported by additional hypothesis.

The parameters describing the typical mesoscopic defects (microcracks, microshears) were introduced in [1] as a localization of the corresponding symmetry group of the distortion tensor. These defects are described by symmetric tensors of the form $s_{ik} = s\nu_i\nu_k$ in the case of microcracks and $s_{ik} = 1/2s(\nu_i l_k + l_i\nu_k)$ for microshears. Here $\boldsymbol{\nu}$ is unit vector normal to the base of a microcrack (normal break) or slip plane of a microscopic shear; $\mathbf{l}$ is a unit vector in the direction of shear ; s is the volume of a microcrack or the shear intensity for a microscopic shear. The microscopic kinetics for the parameter s_{ik} is determined by the Langevin equation

$$\dot{s}_{ik} = K_{ik}(s_{lm}) - F_{ik}, \tag{1}$$

where $K_{ik}(s_{lm})$ and F_{ik} are, respectively, the deterministic and random parts of the force field and satisfy the relations $\langle F_{ik} \rangle = 0$ and $\langle F_{ik}(t_c) F_{ik}(t) \rangle = Q\,\delta(t - t_c)$. Here Q is the correlation function of the fluctuating forces (non-equilibrium potential determining the energy relief of the initial structure). The size and orientation distribution function $W(s,\nu,l)$ of the defects in the phase space of the states is given by the Fokker-Planck equation

$$\frac{\partial}{\partial t}W = -\frac{\partial}{\partial s_{ik}}K_{ik}W + \frac{1}{2}Q\frac{\partial^2}{\partial s_{ik}\partial s_{ik}}W \qquad (2)$$

The energy of these defects, which consist of dislocation pile-ups, can be written in the form

$$E = E_0 - H_{ik}s_{ik} + \alpha s_{ik}^2 \qquad (3)$$

and includes a term $H_{ik}s_{ik}$ that reflects the interaction of defects with an external field and between defects. The "effective field" H_{ik} is written as a sum of an external stress field and the mean-field produced by the defects: $H_{ik} = \gamma\sigma_{ik} + \lambda p_{ik}$, where σ_{ik} is the macroscopic stress tensor, $p_{ik} = n\langle s_{ik}\rangle$ is the macroscopic microdefect density tensor, n is the microdefect density, and λ and γ are parameters of the material. The quadratic term αs_{ik}^2 in Eqn (3) reflects the energy fluctuation arising in the immediate vicinity of a defect as a result of the development of the defect.

In [3] the process of damage accumulation was described assuming the self-similarity of microdefects distributions at the various failure stages (Fig.1)

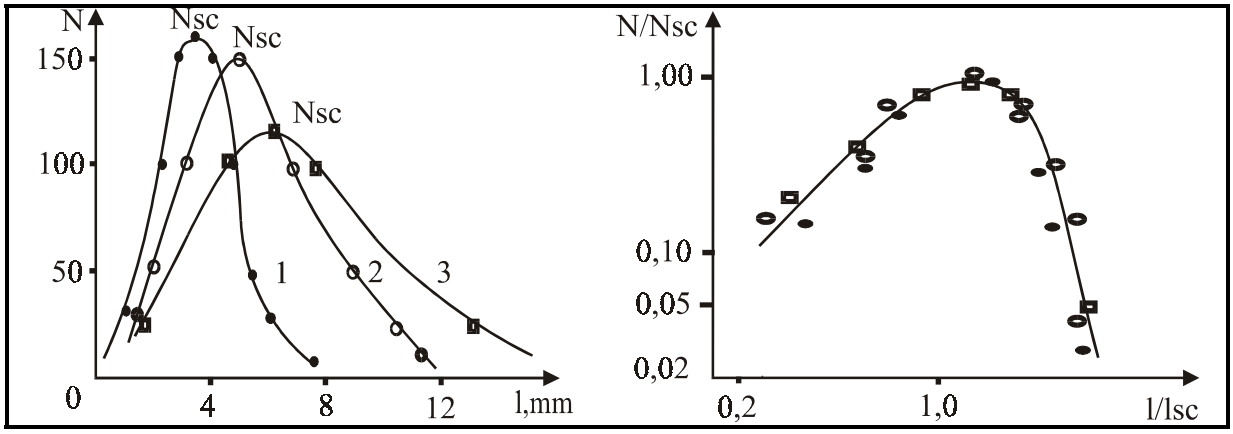

Fig. 1. The distribution of cavities in concentration N and size l in iron during the deformation (creep, stress 9.3 MPa) at temperature 700°C in dimension (N,l) and self-similar (N/N_{sc}, l/l_{sc}) coordinates: 1 - $\varepsilon = 2.1\%$; 2 - $\varepsilon = 6.2\%$; 3 - $\varepsilon = 9.3\%$, [3].

The statistical self-similarity of defect distribution reflects the important from our point of view fact that the distribution function $W(s,v,l)$ has a steady-state form for different time given by the stationary solution of the Fokker-Plank equation with the parametrical dependence of the distribution on some parameter of the self-similarity. The temporal kinetics for this parameter could characterize the formation of the self-similar pattern in the defects ensemble and the change of the specific energy of the system in the course of the creation of the pattern for new scale level in the mesodefects ensemble. This parameter can include two characteristic scales for the defect system: characteristic size of defects and the mean distance between defects. The analysis of experimental data showed that self-similarity of defect accumulation processes may be observed in essentially distinguishing conditions of material deformation.

The qualitative interpretation of the self-similarity hypothesis suggests that geometrical pattern of the defect distribution at the late evolution stage represents magnification of this

pattern existing at the earlier stage. Thus, the self-similarity allows us to introduce in consideration the average dimensions of defects and their energy characteristics and to establish their correspondence to the applied loading.

The solution of the Fokker-Planck equation based on the assumption of statistical self-similarity of the defect distribution [6] makes it possible to represent the distribution function in the form of the steady-state solution, $W = Z^{-1}\exp(-E/Q)$, where Z is a generalized partition function. The parameter Q characterizes the energy relief of the initial structure (grain boundary energy, energy of dislocation pile-ups, influence of the precipitates) representing the microcrack nuclei. This case is valid for the quasi-brittle damage, which is accompanied by the change of the mean size of microcracks. For the damage accumulation under the ductile failure the self-similarity assumption may also be extended if we introduce the spectrum of Q_i for ensembles of defects of each mesoscopic levels. Experimental data presented in [3] support this assumption. The macroscopic magnitude p_{ik} of the defects density is determined by averaging:

$$p_{ik} = n\int s_{ik}\ W(s,\mathbf{v},\mathbf{l})\ \ ds\ \ d^3\mathbf{v}\ \ d^3\mathbf{l} \tag{4}$$

Figure 1 shows p_{xz} versus σ_{xz} for the case of the uni-axial tension for different values of the parameter $\delta = 2\alpha/\lambda n$. The parameter δ is determined by two characteristic scales: the characteristic size l_n of the nucleus of a mesoscopic defect and the average distance l_c between defects. The dislocation model of mesoscopic defects [3] gives $\alpha \approx G/V_0$, where G is the shear modulus and V_0 is the initial "free" volume (volume of the nucleus). Estimating the mean-field constant as $\lambda \approx G$ gives $\delta \approx l_c/l_n$. The solution of Eqn (4) shows that transitions to equivalent classes of curves in Fig. 1 occur when the parameter δ reached critical values δ_* and δ_c, which are bifurcation points. The curves in Fig. 2 correspond to the characteristic responses of a material to a change in the basic modes describing an ensemble of defects. The solid lines in Fig. 2 show the "thermodynamic" branches [7] corresponding to minima of the free energy. The points $P(\sigma^c_{xz}, p^c_x)$ and $S(\sigma^t_{xz}, p^t_{xz})$ are points of a transition to the "dynamical" branches.

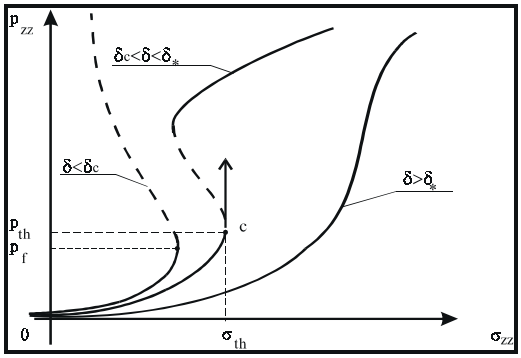

Fig. 2. Nonlinear solid responses on microcrack growth

This statistical description allow us to determine the characteristic solid responses caused by defects. The regimes are defined by two internal scales: characteristic scale of structural heterogeneity l_g (size of grains, blocks) and correlation radius l_c of interaction between defect. Three responses of material to the defect growth were established: monotonous

$(\delta > \delta_*)$, metastable $(\delta_c < \delta < \delta_*)$ and unstable $(\delta < \delta_c)$; δ_* and δ_c being the bifurcation points correspond to the change of the asymptotes. The monotonous response $(\delta > \delta_*)$ is characteristic of a weak interaction between defects. In metastable area the jump-like change of p_{ik} corresponds to the orientation ordering of the mesodefect ensemble. The pass over the δ_c-asymptotic leads to the infinite jump of p_{ik}. The passes over the asymptotics can be recognized as topological transitions that lead to the symmetry changes due to the new organization in the defect system. The free energy F reflecting the spectrum of the solid responses on the defect growth (Fig.1) can be represented as the expansion

$$F = \frac{1}{2}A(1-\frac{\delta}{\delta_*})p_{ik}^2 + \frac{1}{4}p_{ik}^4 + \frac{1}{6}C(1-\frac{\delta}{\delta_c})p_{ik}^6 + D\sigma_{ik}p_{ik} + \frac{1}{2}\chi(\nabla p_{ik})^2 , \qquad (5)$$

where *A,B,C* and *D* are the parameters of the expansion. Taking in view the polar character of the defect interaction the gradient term was introduced that allowed us to describe the nonlocality effect in a "long-wave approximation", χ is the nonlocality coefficient. The forms of the coefficients upon the quadratic term and the higher term provide a qualitative changes of material responses on the defect growth in bifurcation points δ_* and δ_c.

Taking in view that the driving force of the microcrack growth kinetics is the free energy release, we obtain as the consequence of the evolution inequality (Ginsburg-Landau approach) $\frac{\delta F}{\delta T} = \frac{\delta F}{\delta p_{ik}}\dot{p}_{ik} \le 0$ ($\frac{\delta}{\delta p_{ik}}$ is the variation derivative) the kinetic equation for the microcrack density tensor p_{ik}

$$\frac{dp_{ik}}{dt} = -\Gamma\frac{\partial F}{\partial p_{ik}} + \frac{\partial}{\partial x_l}\left(\zeta\frac{\partial p_{ik}}{\partial x_l}\right), \qquad (6)$$

where Γ is the kinetic coefficient, $\zeta = \Gamma\chi$. Using the potential $\Phi = F - \sigma_{ik}\varepsilon_{ik}$ for that the independent variables are σ_{ik} and p_{ik}, and the determination of deformation tensor $\varepsilon_{ik} = -\frac{\partial\hat{0}}{\partial\sigma_{ik}}$ we obtain the equation for the total deformation

$$\varepsilon_{ik} = \frac{1}{2\mu}\sigma'_{ik} + \frac{1}{2k}\sigma_l\delta_{ik} + Dp_{ik}. \qquad (7)$$

The equations (6), (7) represent the system of the constitutive equations of quasi-brittle solid with microcracks.

The transitions over the bifurcation points δ_c and δ_* lead to the sharp change of the symmetry of the distribution function caused by the different interaction of the scalar and the tensor modes of defects with external stress field depending on the value of δ (the size of the defect nuclei r that is determined by the characteristic size of structural heterogeneity and correlation radius of the internal stress field providing the interaction between defects). Studying the kinetic equation (6) with the free energy in the form Eqn (5) we consider the type of the solutions for the condition of the simple tension $\sigma = \sigma_{zz}$ when p_{ik} has only one component $p_{zz} = p$. The analysis of the defect evolution may be carried out due to the study of the heteroclinic solution of the equation

$$Dp + A_0(1-\delta/\delta_*)p + Bp^3 - C_0(1-\delta/\delta_*)p^5 + \frac{\partial}{\partial x}\left(\zeta\frac{\partial p}{\partial x}\right) = 0. \qquad (8)$$

The behavior of such solution can be visualized on the phase portrait (Fig.3). When $\delta > \delta_*$ solution has the form of the spatial-periodical distribution $p \to p\cdot\exp(i\phi)$. When $\delta \to \delta_*$ Eqn (8) changes locally from elliptic to hyperbolic (separatrix S_2) and periodical solution is transformed to the solitary wave solution that corresponds to the diverge of the internal size Λ as $\Lambda \sim -\ln(\delta - \delta_*)$, (Fig.4).

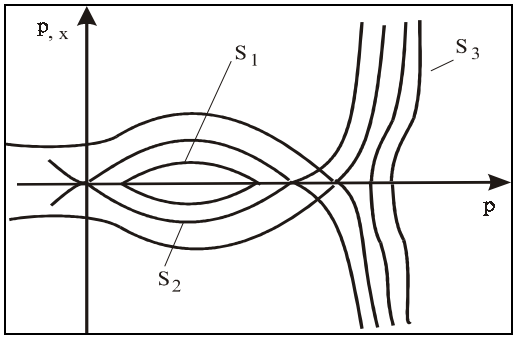

Fig.3: Heteroclinic solution.

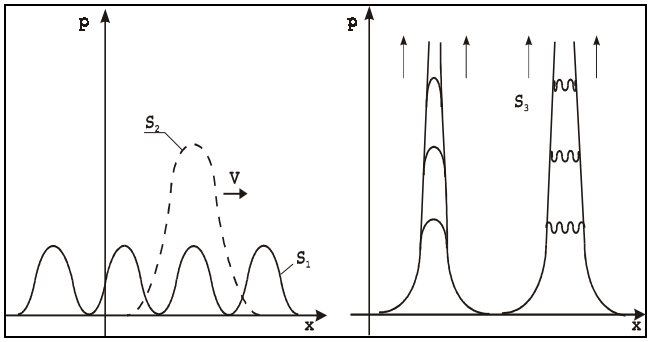

Fig.4: Spatial-time structures in defect ensembles.

The pass over the bifurcation point δ_c (separatrix S_3) gives the qualitative new type of spatial-temporal structures which are characterized by the explosive-like kinetics (peak regimes [9]) of the p-growth over some spectrum of spatial scales (Fig.4.). Let us consider the specific features of nonlinear system for $\delta \le \delta_c$ passing the instability threshold p_c (Fig.1). In this case the p-growth is governed by the difference in the orders of higher terms of expansion for free energy, Eqn (5). Assuming the power law for the nonlocality parameter $\zeta = \zeta_0(p_c)\bar{p}^\beta$ the kinetic equation for p can be written in the form

$$\frac{\partial p}{\partial t} \approx S(p_c)\bar{p}^\omega + \frac{\partial}{\partial x}\left(\zeta_0(p_c)\bar{p}^\beta\frac{\partial \bar{p}}{\partial x}\right) \qquad (9)$$

where $\bar{p} = p/p_c$ (in the following the "hat" is dropped), $\omega = 5/3$. It was shown in [4] that the developed stage of p-growth exists as the self-similar solution for $t \to t_c$ and can be represented in the form

$$p_A = q(t)f(\xi), \quad \xi = \frac{x}{\phi(t)}, \quad g(t) = G\left(1 - t/t_c^i\right)^{-m} \qquad (10)$$

where $g(t)$ governs the growth law of over the spectrum of the scales ζ_i (the eigen-value spectrum); φ defines the half-width evolution of the localization area; $G > 0$ and $m > 0$ are the parameters combined from the parameter of Eqn (9).

EXPERIMENTAL INVESTIGATION OF CRACK PROPAGATION.

Various techniques can be used for investigation of crack propagation dynamics. One of them [5,7] provides good accuracy with high resolution in time for the determination of crack propagation velocity. This technique is used to study the statistical features of crack propagation. The propagating crack cuts a thin metallic film on the surface of a specimen thus changing the film electric resistance. By measuring this resistance one can determine the coordinate of the crack tip. Another experimental technique is based on high speed photography of the propagating crack. This technique allows us to obtain stress distribution and stress intensity in the specimen using the photoelasticity or shadow method [7].

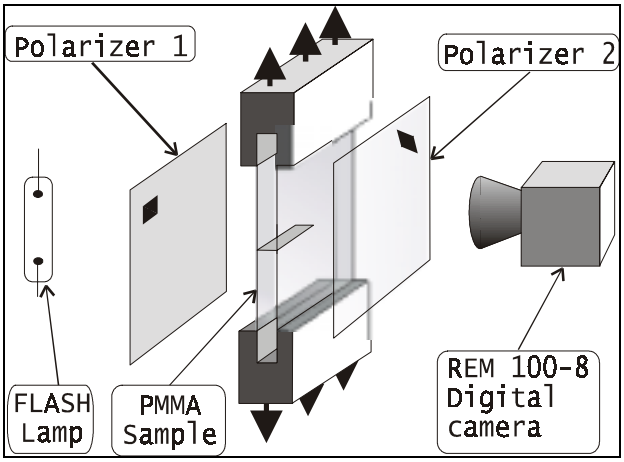

Fig.5: Experimental setup

In our experiments we use rectangular PMMA specimens with length L of 141 mm, height 66 and 86 mm and thickness varied from 0.6 to 1.9 mm. PMMA constants are: $E=6.0GNm^{-2}$, $\nu=0.33$, $\rho=1.18g\ cm^{-3}$. The Rayleigh wave speed is 1400m/s. Stress was varied from 13 to 45 MPa.

The scheme of experimental setup is presented in Fig.5.

The experimental apparatus consists of a loading device to provide strain up to 10^{-2}, a high speed camera to record the stress field and a synchronising device. We measure the force applied to the sample, the mean crack speed and the stress field in the specimen. Finally we investigate the fracture surface. In most experiments the crack was initiated in the middle of the specimen short side by a sharp blade. Fracture is performed by applying force in the plane of the sample and parallel to the shortest side of the plane.

We study the stress evolution using the photoelasticity method. With the high speed digital camera Remix REM 100-8 provided by LAMEF (ENSAM France) eight pictures with resolution 740x574 were recorded. Time lag between two pictures was 10 or 5 μs.

The crack velocity was measured in two ways: Knowing the crack length on each picture and time lag between pictures one can obtain the mean crack velocity. Another method is based on the Doppler effect. We study the acoustic waves generated by the crack and propagating forward (ν_1,λ_1) and backward (ν_2,λ_2). By measuring the wavelength difference we obtain the crack speed

$$V=\frac{\lambda_2-\lambda_1}{\lambda_2+\lambda_1}V_R=\frac{\nu_1-\nu_2}{\nu_1+\nu_2}V_R, \qquad (11).$$

where V_R is the speed of the emitted waves; V_R is obtained by measuring the propagation rate of the wave front. We have carried out experiments on interaction between the moving crack and holes in the sample. During this interaction the crack produces a single pulse and in certain experiments the crack arrest is observed. It is easy to identify the position of the pulse front in each picture and to obtain the velocity of acoustic waves in the specimen for given loading and frequency range. The crack generates stress waves at the velocity of 1400±100 m/s close to the dynamic Rayleigh wave speed V_R^* [6]. Both methods are in good agreement. The discrepancy between results is about 7-8 %.

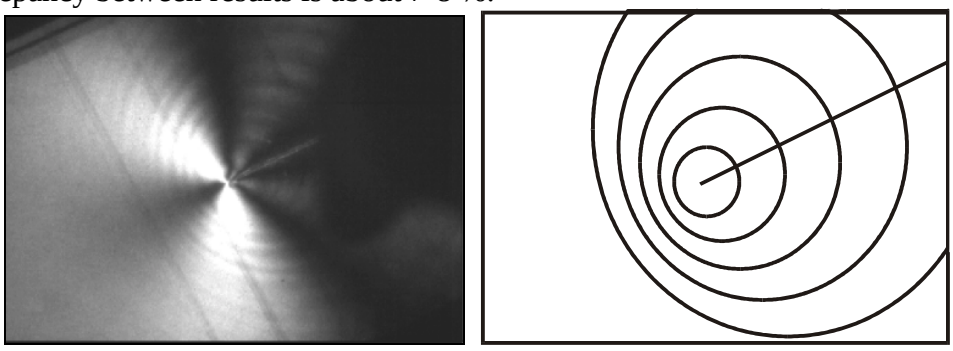

Fig.6: Wave pattern and scheme of process.

Experimental results

The crack propagates in two regimes: steady-state and branching (Fig. 7).

i) In the steady-state mode the crack propagates at a low speed (up to 416 m/s or 0.3 V_R) and produces the smooth surface.

ii) In the branching mode the crack velocity is higher: 500-800 m/s (0.36-0.6 V_R).

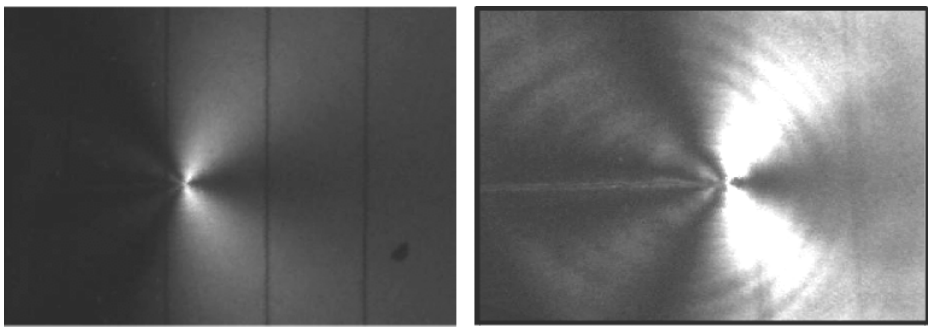

Fig.7. Stress field produced by slow (left) and fast (right) cracks.

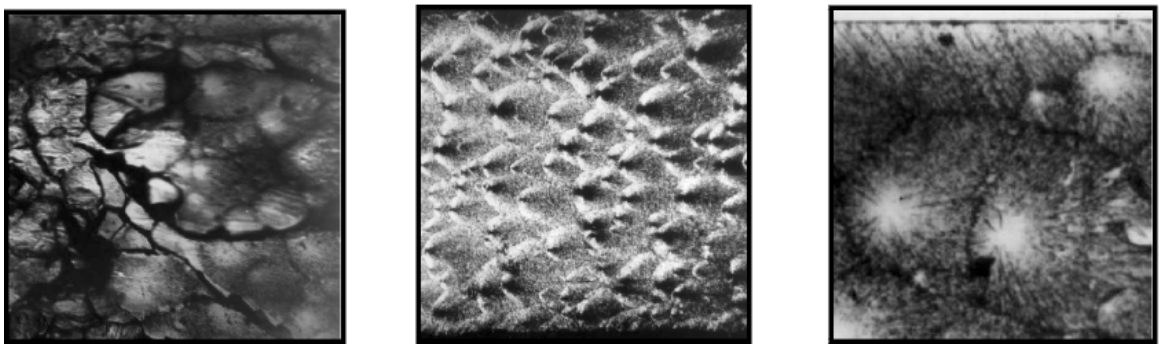

a b c

Fig. 8: Typical fracture pattern for the crack velocity: a- 600 m/s, b, c - 400 m/s. Magnification is a,b - x 60; c - x 600.

The fracture surface generated by the fast crack consists of “mirror” zones, Fig.8. These zones correspond to the daughter cracks in the process zone near the crack tip. The location of these zones depends on the crack speed. When the speed is low, the zones are in the same plane (the smooth crack surface), at high velocities they have different orientation, which corresponds to the high roughness of the crack surface. The crack surface roughness depends on the crack speed. At velocities exceeding 650 m/s the macrobranching appears.

INSTABILITY MECHANISM UNDER CRACK PROPAGATION

Let us apply the developed approach concerning the spatial-time kinetics of the microcrack ensemble evolution to the study of the mechanisms that govern the dynamics of crack propagation. It is obvious now that the process of the interaction of the main crack and the surrounding microcrack ensemble includes two stages. The first is the formation of the defect distribution in the process zone at the crack's tip, which provides the creation of the damage localization areas with qualitative new properties. It means the formation of the new defect structure with the radius of the own stresses reaching the main crack that provide the sensitivity of the main crack to the new structural defect at the scale level corresponding to the main crack. The kinetics of the microcrack ensemble involves the generation of new scales in the process zone in the form of the dissipative structures with the peak regime kinetics on the fundamental length .The solution of Eqn 9 contains two parameters: the fundamental length L_T and the "peak time" t_c. The peak time t_c represents a sum of two times: t_1 is the period of the formation of the spatial defect distribution that is close to self-similar one, and t_2 is, the so-called, focusing time [8]. These two parameters determine the critical velocity of the crack propagation $V_c \approx \frac{L_T}{t_c}$. Now we consider in more detail the crack propagation under the conditions (external stress and initial crack length), which are responsible for the steady state ($V < V_c$) and crack branching ($V > V_c$) scenario. The steady state propagation in the direction of the main crack is realized for external conditions providing the creation of the self-similar profile of microcrack distribution along the main crack when the crack speed doesn't exceed the critical one V_c. It means that in the process zone at the crack tip the stress distribution $\sigma > \hat{\sigma}_c$ is formed on the scale L_T and there exists the time period $t = \frac{L_T}{V} \geq t_c$ for nucleation of a new daughter crack along the trace of the main crack. For the velocities $V > V_c$ this is impossible, since $\frac{L_T}{V} < t_c$. However, taking into account the asymptotic law of stress distribution at the crack tip $\sigma_{ij} \approx K_I r^{-\frac{1}{2}} f_{ij}(\theta)$ (here K_I is the stress intensity factor; r, θ are the coordinates of points in the process zone), we can determine the branching angle θ_* for which the external conditions defined by the value of $K = K_I^*$ (external stress and current length of the main crack) provide the existence of L_T and $t = t_c$ $f_{\theta\theta}(\theta_*) = \hat{\sigma}_c K_I^{*-1} L_T^{\frac{1}{2}}$. For the given value of K_I^*, the values of the angles $0 < \theta < \theta_*$ are excluded since the condition for the corresponding traces $t < t_c = \frac{L_T}{V_c}$ doesn't allow the formation of the self-similar profile of the microcrack distribution (daughter cracks). The next important question is what mechanism governs the increase of the main crack speed in the range $V > V_c$ when the rate of the

interaction of the main crack with the closest daughter crack is limited by V_c. As it follows from the consideration of the scaling for the spalling [4], the reason is the excitation of the numerous "peak regime structures" when the scale of the process zone L_{pz} with $\sigma > \hat{\sigma}_c$ expands as $L_{pz} \approx L_T k$, where $k = 1,2 \ldots$ The nucleation of these structures on the total length $L_T k$ (complex structures [1]) can be considered as the subjection of the system behavior to new attractor which is determined in the set of new independent coordinates, that is in the set of the structures of the various complexity obtained from the self-similar solution. (10). This leads to the sharp change of the symmetry properties of the system that was predicted in [10].

The authors are kindly indebted to Professor J-L.Lataillade for the opportunity of the experimental study at LAMEF-ENSAM and the supportive discussions.

REFERENCES

[1] Naimark, O.B. *On thermodynamics of deformation and fracture of solids with microcracks*. Institute of Mechanics of Continuous Media, USSR Academy of Sciences, Sverdlovsk (in Russian), 1982.

[2] Naimark, O.B., Davydova, M.M., & Plechov, O.A. *Failure scaling as multiscale instability in defect ensemble.* Proceedings of NATO Workshop "Probamat-21 Century", Kluver, 127-142, 1998.

[3] Botvina, L.R., Barenblatt, G.I. *Self-similarity of damage accumulation*, Problems of Strength, 17-24, n.12, 1985.

[4] Naimark, O.B. *Kinetic transition in ensembles of microcracks and some nonlinear aspects of fracture.* In Proceedings of the IUTAM Symposium on nonlinear analysis of fracture, in J.R.Willis (eds.), Kluver, The Netherlands, 285-298, 1996

[5] Sharon E., Gross, S.P., Fineberg J. *Local crack branching as a mechanism for instability in dynamic fracture,* Phys. Rev. Lett **74,** 5097-5099,1995.

[6] Marder, M. & Gross, S. *Origin of crack tip instabilities.* J. Mech. Phys. Solids. **43**, 1, 1-48, 1995.

[7] Boudet, J.F., Ciliberto, S. & Steinberg, V. *Dynamics of crack propagation in brittle materials,* J. Phys. II France, **6,** 1493-1516, 1996.

[8] J.F. Kaltoff, J. Beinert, and S. Winkler, *Analysis of fast running and arresting crack by the shadow-optical method of caustics,* IUTAM Symp. Opt. Methods Mech. Solid (A. Lagarde, Ed.), University of Poitiers, France, Sept. 10-14, 1979, Sijthoff-Noordhoff, Alphen aan den Rijn, The Netherlands, 1980, pp 497-508.

[9] Beljaev, V.V. & Naimark, O.B. *Kinetics of multicenter fracture under shock wave loading.* Sov. Phys. Dokl., **312**, n. 2, 289-293,1990.

[10] Naimark, O.B. *Structural Transitions in Solids and Mechanisms of Plasticity and Failure.* Preprint of the Institute of Continuous Media Mechanics of the Russian Academy of Sciences, Perm, 1995.